Sorting out abrasion in a gypsum dune field

Douglas J. Jerolmack,[1] Meredith D. Reitz,[2] and Raleigh L. Martin[1]

Received 19 July 2010; revised 26 January 2011; accepted 2 February 2011; published 12 April 2011.

[1] Grain size distributions in eolian settings are the result of both sorting and abrasion of grains by saltation. The two are tightly coupled because mobility of particles determines abrasion rate, while abrasion affects the mobility of particles by changing their mass and shape; few field studies have examined this quantitatively. We measured grain size and shape over a 9 km transect downwind of a line sediment source at White Sands National Monument, a gypsum dune field. The sediment source is composed of rodlike (elongate), coarse particles whose shapes appear to reflect the crystalline structure of gypsum. Dispersion in grain size decreases rapidly from the source. Coarse particles gradually become less elongate, while an enrichment of smaller, more elongate grains is observed along the transect. Transport calculations confirm that White Sands is a threshold sand sea in which (1) the predominant particle diameter reflects grains transported in saltation under the dune-forming wind velocity and (2) smaller, elongate grains move in suspension under this dominant wind. Size-selective transport explains first-order trends in grain size; however, abrasion changes the shape of saltating grains and produces elongate, smaller grains that are spallation and breaking products of larger particles. Both shape and size changes saturate 5–6 km downwind of the source. As large particles become more equant, abrasion rates slow down because protruding regions have been removed. Such asymptotic behavior of shape and abrasion rate has been observed in theory and experiment and is likely a generic result of the abrasion process in any environment.

Citation: Jerolmack, D. J., M. D. Reitz, and R. L. Martin (2011), Sorting out abrasion in a gypsum dune field, *J. Geophys. Res.*, *116*, F02003, doi:10.1029/2010JF001821.

1. Introduction

[2] The mass of a particle is the principle determinant of its mobility for a given range of flows. Particle diameter is typically the most important grain parameter because it varies several orders of magnitude more than density for most natural sediments. In addition, the shapes of particles contain information about their mode of transport and may also affect their mobility. It is well known that eolian environments contain mostly well-sorted, subrounded grains due to both size-selective transport and saltation abrasion [e.g., *Bagnold*, 1941; *Kuenen*, 1960; *Goudie and Watson*, 1981; *Mazzullo et al.*, 1986]. It is increasingly being recognized that a smaller population of angular grains carried in suspension (dust to fine-sand size) may be the products of chipping and breaking of saltating grains [*Rogers and Schubert*, 1963; *Smalley and Vita-Finzi*, 1968; *Wright and Smith*, 1993; *Wright*, 2001; *Bullard et al.*, 2004, 2007; *Crouvi et al.*, 2008, 2010; *Jerolmack and Brzinski*, 2010]. The highly energetic collisions typical of eolian transport mean that abrasion may be a significant process for all grains in saltation. Grains carried in suspension interact little with the bed while their diminutive size means that collision energy is reduced, so abrasion is likely unimportant [*Kuenen*, 1960; *Bullard et al.*, 2004; *Jerolmack and Brzinski*, 2010]. The relationships between grain mobility and abrasion present the possibility for a fascinating but little explored feedback: the frequency and magnitude of saltation should strongly control abrasion rate, while continued abrasion changes the mobility of particles by altering grain size and shape. Exploring this feedback in a natural dune field forms the main topic of this paper.

[3] Models for saltation abrasion and eolian erosion typically follow the form that abrasion rate scales with the kinetic energy of impact of particles [*Anderson*, 1986], and therefore their diameter cubed and velocity squared. It is clear that the coefficient of proportionality in such a relation must be related to the hardness or brittleness of the material [*Kuenen*, 1960; *Lewin and Brewer*, 2002]. *Kuenen* [1960] also found, however, that abrasion rate was positively related to "angularity" in his experiments. Quantitative studies isolating the effect of grain shape on abrasion were only undertaken recently. *Durian et al.* [2006] conducted a series of experiments in which two-dimensional dry-clay "pebbles" were abraded by collision with the walls of a rotating square drum. Because the pebbles were homogeneous in composition with no crystal structure, the effect of shape on particle abrasion could be isolated. The initially square particles progressively became more circular with time, with protruding regions of

[1]Department of Earth and Environmental Science, University of Pennsylvania, Philadelphia, Pennsylvania, USA.
[2]Department of Physics and Astronomy, University of Pennsylvania, Philadelphia, Pennsylvania, USA.

0148-0227/11/2010JF001821

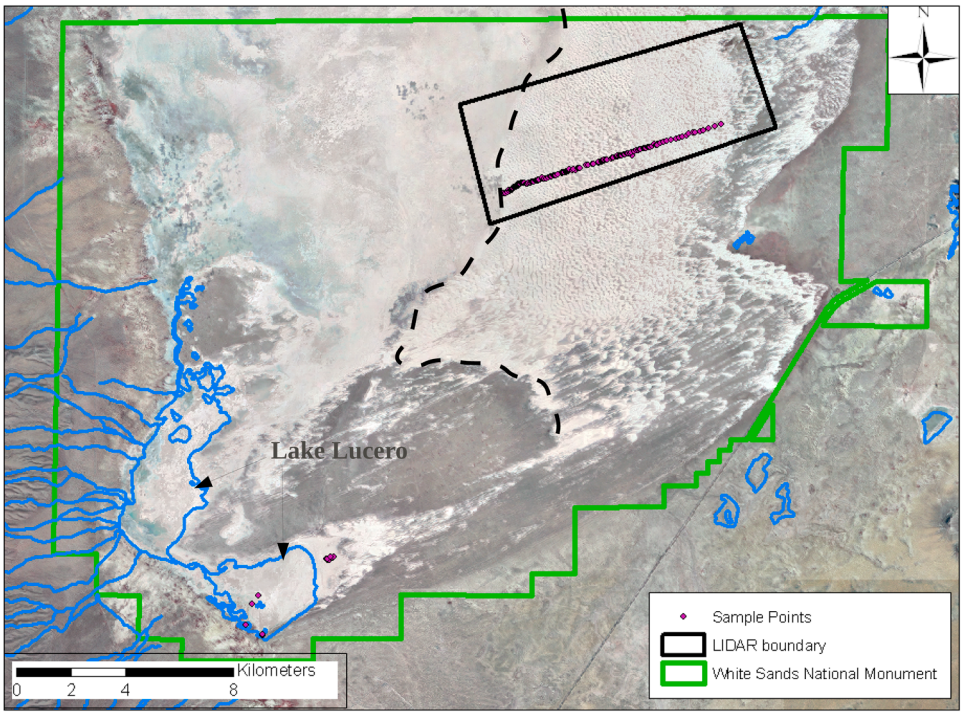

Figure 1. Eastern side of the Tularosa Basin, with channels and White Sands National Monument boundary shown. The deflation basin is the featureless flats on the left half of the image, while the dune field abruptly begins approximately midway across the image. LiDAR boundary and surface sediment sample locations are indicated. Dashed line shows approximate upwind boundary for the dune field, which is the sediment source. Lake Lucero is indicated.

high curvature preferentially chipping off. Abrasion rate slowed with time, however, and particle shape asymptotically approached a limiting value that was not circular. This behavior was reproduced by numerical models in which sequential spallation (chipping off) occurred by random removal of corners [*Durian et al.*, 2007; *Krapivsky and Redner*, 2007].

[4] It appears that abrasion rate of natural particles under saltation depends on three main factors: (1) mobility, (2) material strength, and (3) shape. Experiments with quartz sand demonstrate that abrasion products are not infinitesimal. Under conditions representative of eolian saltation, discrete, angular dust- to fine-sand-sized particles were formed through spallation of sand [*Bullard et al.*, 2004; see also *Crouvi et al.*, 2008, 2010]. This is similar to the "corner chipping" observed in the experiments of *Durian et al.* [2006]. Under more energetic conditions, sand can actually be broken or crushed into smaller particles [*Wright and Smith*, 1993], although these conditions are not likely to be common in quartz-rich sand seas.

[5] There are conflicting accounts of the significance of abrasion versus size-selective transport (sorting) for determining the grain size distributions in actual desert dune fields [*Mazzullo et al.*, 1986]. One reason is that field studies providing high spatial resolution data of grain size and shape over sufficient distances have not been carried out. In order to enhance the probability of detecting grain abrasion processes over a shorter distance, we carried out just such a field study in the gypsum dune field at White Sands National Monument. The goal of this paper is to delineate the relative contributions of sorting and abrasion in controlling spatial changes in grain size distribution along a downwind transect. In addition, we seek to relate sorting and abrasion to sediment transport mechanics in a manner that is generalizable to other dune fields, despite the specific mineralogical and transport conditions at White Sands. This requires reducing the time varying wind velocities to a single representative value (the "dune-forming wind" [*Jerolmack and Brzinski*, 2010]) and parameterizing complex grain size and shape distributions using a small set of variables.

2. Background

[6] Field work was conducted in White Sands National Monument. The dune field covers ~400 km^2 of the Tularosa Basin in southern New Mexico, making it the world's largest gypsum dune field. Pleistocene Lake Otero formerly occupied most of the basin; however, increased aridity due to Holocene climate change resulted in retreat of the lake and exposure of gypsum evaporites (Figure 1) [*Langford*, 2003; *Kocurek et al.*, 2007; S. Fryberger, Geological overview of White Sands National Monument, http://www.nps.gov/archive/whsa/Geology%20of%20White%20Sands/GeoHome.html, 2009]. The western side of the basin has experienced deflation (wind erosion), supplying the gypsum sand that makes up the dunes to the east (Figures 1 and 2). There is mounting evidence that deflation may have been episodic: (1) two old lake shorelines have been identified, with the outer shoreline older than the inset shoreline, and (2) regional deflation events in other locations have been

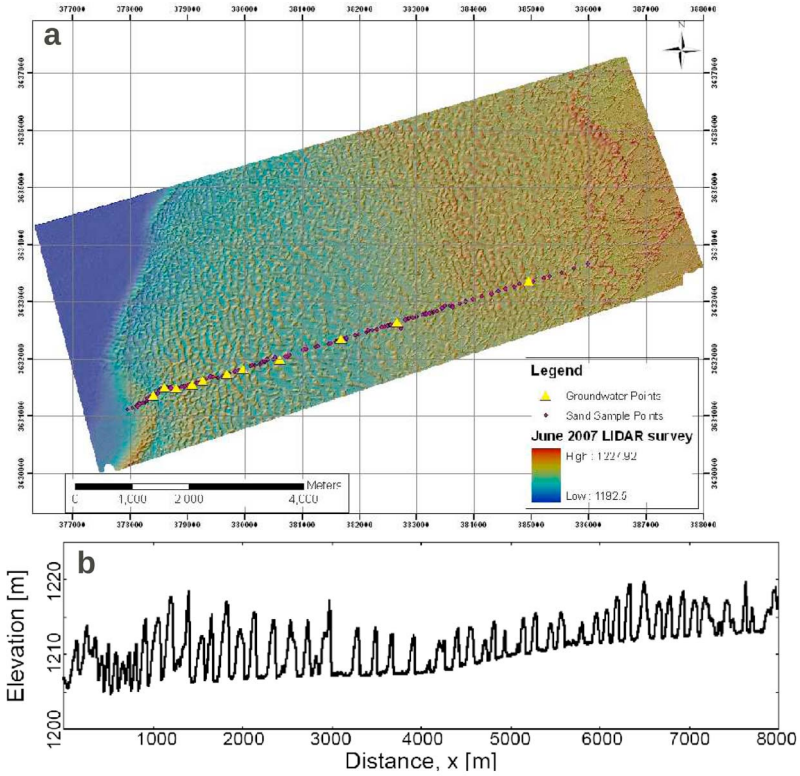

Figure 2. Elevation data for White Sands. (a) LiDAR map from June 2007, courtesy of Gary Kocurek (University of Texas-Austin). Sediment source is the ridge in the left side that runs approximately N-S. Transect is indicated by purple dots showing locations of surface samples. UTM coordinates are shown. (b) LiDAR topography showing the elevation profile located approximately along the sampled transect.

dated to ~7 ka and ~4 ka [*Langford*, 2003]. Although age constraints at White Sands are insufficient, available dates and morphologic degradation of shorelines are consistent with the two major deflation events identified in the region. It is likely that formation of the dune field was initiated during the first major deflation event ~7 ka [*Langford*, 2003]. It is unclear whether sediment has been supplied to the dune field continuously, or primarily during periods of major deflation. *Langford* [2003] suggests that the modern source of sediment to the dune field is the edge of the deflation basin.

[7] Although winds are variable at White Sands, the prevailing wind direction is from the southwest [*Kocurek et al.*, 2007; Fryberger, http://www.nps.gov/archive/whsa/Geology%20of%20White%20Sands/GeoHome.html, 2009]. The transverse orientation of dune crestlines to the prevailing winds supports the interpretation of a dominant, unimodal wind regime. In this paper we will consider "downwind" to mean in the direction of dune migration and hence net sediment transport, which is about 25°N of east (see section 3.2). The dune field begins abruptly with a large sediment ridge (Figures 1 and 2). Downwind of this sediment source, dunes become more sparse until a distance of about 6–7 km, when the aerial density of dunes increases slightly again (Figure 2a). This subdued ridge, located downwind of a subtle rise in topography (Figure 2b), may represent a small, secondary source of sediment to downwind dunes.

[8] Spatial dune patterns at White Sands reflect changes in the availability and transport rate of mobile sediment downwind [*McKee*, 1966; *McKee and Douglass*, 1971; *Reitz et al.*, 2010; *Ewing and Kocurek*, 2010a]; moving from west to east, transverse dunes and crescentic ridges transition to isolated barchan dunes, and eventually give way to parabolics when transport rate becomes low enough that vegetation can colonize [*Reitz et al.*, 2010]. Average dune migration speed is 1–3 m/yr, while characteristic dune height and spacing are ~5 m and ~150 m, respectively [*Ewing et al.*, 2006; *Kocurek et al.*, 2007; *Reitz et al.*, 2010; *Ewing and Kocurek*, 2010a]. There are spatial trends in these dune parameters downwind, but they are not the focus of this paper. The water table at White Sands is close to the surface, such that flat interdune areas are moist even in summer. This is associated with sediment accumulation within the interdunes and partial cementation of the gypsum dunes [*McKee*, 1966; *Kocurek et al.*, 2007; Fryberger, http://www.nps.gov/archive/whsa/Geology%20of%20White%20Sands/GeoHome.html, 2009], both of which limit sediment mobility.

[9] White Sands is nearly ideal for this study for three reasons: (1) the line source of sediment at the upwind dune margin presents a well-defined boundary condition [cf. *Ewing and Kocurek*, 2010b] for transport down wind; (2) a strongly dominant wind direction ensures that transport distance of an individual grain is closely approximated by its distance downwind of the line sediment source; and (3) the wide range of grain sizes present at the source, combined with the

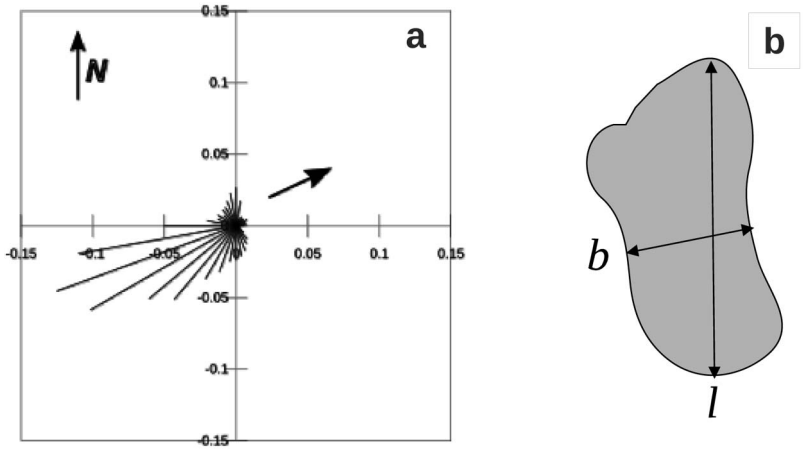

Figure 3. (a) Wind rose of excess shear velocity, $(u - u_{*c})$, measured from time series at Holloman Air Force base. North is indicated. Diagonal arrow shows vector sum, indicating a dominant sediment transport direction of 25°N of east. Note that dunes are actually oriented transverse to a slightly different angle, 35°N of east, indicating an offset between net transport direction and dune orientation. This is likely due to the seasonality of winds of different magnitudes, in which the dunes are oriented to the strongest spring winds and slightly modified by weaker secondary winds from a different direction. (b) Planar projection of a grain, showing the short (b) and long (l) axes. Elongation is the measure of the ratio l/b, while the nominal grain diameter (d) measured by the Camsizer is $d \approx b$.

soft nature of gypsum sediment, mean that both sorting and abrasion processes should be significant over fairly short distances. While we recognize that such simplifying conditions are not present in many dune fields, they allow us to isolate sorting and abrasion processes that result from sediment transport, and to measure these effects over distances of kilometers. Spatial grain size sorting is expected to occur over individual dunes due to the complex processes of flow separation, avalanching and wind stress variation due to dune shape. It is not our aim to characterize this behavior. Accordingly, we mostly examine variation in grain size and shape that occurs over spatial scales significantly larger than a dune wavelength.

3. Methods

[10] The goal of this study was to determine spatial changes in grain size and shape that result from transport away from a sediment source. The source of sediment is well defined by the linear ridge that runs approximately N-S, forming the western edge of the dune field. We selected a ~9 km transect in the dominant transport direction, beginning at the upwind edge of the dunes and centered on the "Heart of the Sands" loop trail (Figure 1). This transect was located in a swath of airborne Light Detection And Ranging (LiDAR) topographic data, made available to us by the Kocurek group at University of Texas-Austin, over a 10 km × 4 km region in June 2007 and June 2008 (Figure 2a). Grain size data were collected in mid-March 2009, at the beginning of the typical windy season (March to April) at White Sands. Winds during the time of sample collection were oblique to, and even opposing, the dominant transport direction. Such variability may have confounded the downwind sorting we sought to examine; however, as we will see, robust trends could still be found across the length of the dune field.

3.1. Sampling and Grain Size and Shape Analysis

[11] The transect line (Figure 2a) was loaded into a Trimble GeoXH handheld differential GPS. Sediment surface samples were collected at each dune encountered along the transect, in three locations: on the stoss side of the dune at a point ~1 m higher than the elevation of the upwind interdune, at the location of the dune crest, and at the base of the dune lee. This allowed us to explore and correct for local sediment sorting effects over individual dunes, and resulted in almost 150 sediment samples. Due to limited time, only dune crests were sampled for distances beyond ~5700 m from the source. The location of each sample was logged using the GPS. Only loose (noncemented) grains were sampled, using a scoop that penetrated less than 1 cm into the subsurface. Each sample contained approximately 50–100 cm^3 of sediment, which we verified by mineralogical analysis to be nearly 100% gypsum (sediment density, ρ_s = 2380 kg/m^3). Samples were typically taken from areas covered by small (~10 cm wavelength) ripples, and some variation among them may occur from sampling different portions of these ripples. Such variability is not accounted for, but is not expected to affect overall downwind trends.

[12] Sediment size and shape were measured in the laboratory using a Retsch Camsizer (www.retsch-technology.com), which digitally imaged and analyzed hundreds of thousands of particles for each sample. The empirically determined lower detection limit is 0.04 mm, so grains having a smaller diameter were not measured. Errors in size estimation are negligible compared to sieving over the measured range. Sediment grain size distributions were generated from measures of nominal grain diameter d, determined using 40 logarithmically spaced bins over the range 0.05–8 mm. Note that d measured by the Camsizer represents the shortest axis (b) in a planar projection of the grain (Figure 3b), and thus represents the intermediate axis in a typical three-

dimensional description of particle shape. We characterized overall sorting for each sample using a normalized dispersion parameter, $\sigma^* = (d_{90} - d_{10})/d_{50}$, where the subscript indicates the volume fraction of sediment below that size in a sample. The Camsizer has the capability to assess bulk shape characteristics for each grain-size bin. We found that elongation (as opposed to, e.g., sphericity) provided the largest dynamic range among samples, and thus elongation is the quantitative shape parameter reported in this study. Elongation for Camsizer samples is defined as l/b, the ratio of the longest axis (l) to the shortest axis (b) in a planar projection of the grain (Figure 3b). There are more sophisticated algorithms available for describing grain shape [e.g., *Mazzullo et al.*, 1986; *Durian et al.*, 2006]; however, elongation data were automatically measured during grain size analysis and thus were simple to generate. It is also a natural parameter choice to describe gypsum, as crystals often exhibit a rodlike shape whose length is reduced by abrasion during transport. In this paper, we roughly follow grain shape definitions of A. Allaby and M. Allaby (A Dictionary of Earth Sciences, www.encyclopedia.com, 1999): "prolate" refers to rod-shaped particles, while "equant" refers to more square or circular particles with planar aspect ratios approaching one. The word "roundness" often implies smoothness of the grains at a small scale [*Mazzullo et al.*, 1986]. We were not able to quantify roundness of our samples and therefore we use the term qualitatively simply to refer to smaller-scale smoothness, that is, round as the opposite of angular.

3.2. Sediment Transport Capacity and Dune-Forming Wind

[13] It has long been understood that dune sands must generally reflect a population of grains that undergo transport via saltation under the dominant wind conditions [*Bagnold*, 1941; *Warren*, 1979; *Lancaster*, 1985]. *Lancaster* [1985] showed how the combination of magnitude and frequency of occurrence determines the importance of different winds in terms of moving sediment. *Jerolmack and Brzinski* [2010] recently formalized this idea, showing that a dominant or "dune-forming wind," analogous to bankfull flow in rivers, may be determined precisely using the concept of geomorphic work [*Wolman and Miller*, 1960]. This allows the objective derivation of a single representative value for wind shear velocity, u_*, that is responsible for long-term sediment transport and sorting. This formative shear velocity (u_{*f}) is the wind that moves the most sediment in a time-integrated sense. It appears that net sediment transport is well described by a single representative grain size as well; geomorphic work is assessed using the median grain diameter (d_{50}) of surface sediments. The reduction of the time series of wind data to a formative shear velocity is critical for our analysis: a single value for u_{*f} will be used to determine mobility of all grain size classes. This procedure obviously neglects complexities such as spatial variations in winds along the dune field, and temporal fluctuations in stress due to fluid turbulence. We hypothesize that this approach is justified as long as grain size and shape patterns are assessed over distances large enough that such variability averages out, akin to the assumptions associated with a steady, uniform flow approximation. In addition, the method is justified a posteriori by comparing expected grain-size sorting trends to the actual data. Finally, we believe this simplified approach is valuable because it uses widely available meteorological data and requires only limited information from the dune field itself, and so it may be applied to many settings.

[14] In order to determine the direction and magnitude of the dune-forming wind at White Sands, we downloaded wind velocity data from the nearby NOAA National Climatic Data Center weather station at Holloman Airforce Base, station #747320. Data consist of hourly measurements of wind speed and direction, with resolutions of 1 mph and ~10°, respectively, covering the years 1964–2008. Measurements were taken at a height $z = 10$ m above the surface. The first step was to convert measurements of wind speed (u) into shear velocity, using the law of the wall:

$$u(z) = \frac{u}{\kappa} \ln\left(\frac{z}{z_0}\right), \tag{1}$$

where $\kappa = 0.4$ and $z_0 = 10^{-4}$ m is a roughness parameter empirically determined in the field on a dune at White Sands [*Jerolmack et al.*, 2006]. Because we are only concerned with wind events that transport sediment, it is necessary to determine the critical shear velocity for entrainment of grains, u_{*c}. To further simplify the problem, we assume that conditions for aerodynamic entrainment of grains may be calculated (1) independently for each particle size class and (2) without regard to particle shape. Experimental data indicate that grain shape has little impact on critical shear velocity, but grain size heterogeneity has some effect [*Nickling*, 1988]. We expect assumption 1 to result in some unquantified error, but that our mobility estimates will be broadly correct. We employ an empirical function by *Shao and Lu* [2000] that was fit to wind tunnel data over the range $0.05 \le d \le 1.8$ mm:

$$u_{*c} = \sqrt{0.0123\left(\frac{\rho_s g d}{\rho_f} + \frac{3e^{-4}\ \mathrm{kg/s^2}}{\rho_f d}\right)}, \tag{2}$$

where $\rho_f = 1.23$ kg/m^3 is density of air at 20°C and $g = 9.81$ m/s^2 is acceleration due to gravity. The rest of the analysis of dune-forming wind assumes that grains may be represented by a single grain size, the measured median value $d_{50} = 0.4$ mm. The predicted value of u_{*c} for this grain size at White Sands is only 5% different from the observed u_{*c} for onset of motion (Fryberger, http://www.nps.gov/archive/whsa/Geology%20of%20White%20Sands/GeoHome.html, 2009), lending support that (2) may be applied to assess grain mobility. We generated a rose diagram of excess shear velocity ($u - u_{*c}$), which indeed indicates a strong dominance of winds from the southwest (Figure 3a). Sediment transport capacity depends nonlinearly on excess shear velocity. The next step was to compute sediment transport capacity of all wind events for which $u \ge u_{*c}$, using the corrected *White* [1979] formula as presented by *Namikas and Sherman* [1997],

$$q_s = 2.61\frac{\rho_f u^3}{g}\left(1 - \frac{u_{*c}}{u}\right)\left(1 + \frac{u_{*c}}{u}\right)^2. \tag{3}$$

Estimation of the dune-forming wind is not sensitive to the details of (3): any relation of the form $q_s \propto u^3$ will produce similar results. The net annual sand transport vector was

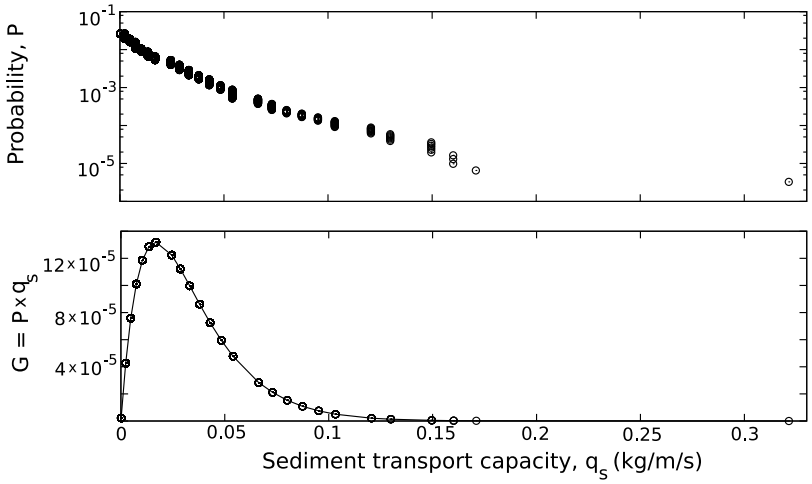

Figure 4. (top) Frequency-magnitude plot of computed (nonzero) sand transport capacity values using ground-based wind velocity records from White Sands, New Mexico. Data were recorded every hour for years 1964–2008, at elevation of 10 m above ground (World Meteorological Organization standard), from Holloman Air Force Base near Alamogordo, New Mexico. Downloaded from National Climatic Data Center (http://www.ncdc.noaa.gov/oa/ncdc.html). Distribution is approximately exponential (note semi-log axes). (bottom) Geomorphic work plotted against sediment transport capacity, using exponential fit to frequency data in Figure 4 (top). Note well-defined peak indicating dune-forming sediment flux of 0.017 kg m^{-1} s^{-1}.

computed [see *Bagnold*, 1941], having a magnitude $q_{s,a}$ = 5 m^2/yr and direction of 25°E of north. Computed annual transport capacity is close to the value estimated using the average migration speed (c = 2.5 m/yr) and elevation ($\langle\eta\rangle$ = 2.1 m) of mobile dunes, $q_s = c\langle\eta\rangle/\varphi$ = 8 m^2/yr, where φ = 0.65 is a representative sediment concentration of the bed. Computed transport direction is also consistent with dune migration patterns.

[15] The values for sediment transport capacity generated from the wind record and (1)–(3) were then ranked to generate a complementary cumulative distribution function, $P(Q_s > q_s)$, which represents the probability P that an observed transport event Q_s is larger than the magnitude q_s. The data are well fit by an exponential function,

$$P(Q_s > q_s) = e^{-q_s/\langle q_s\rangle}, \tag{4}$$

where brackets indicate the average value for the series. *Jerolmack and Brzinski* [2010] defined the distribution of geomorphic work (G) as the product of the magnitude of a given transport event and its frequency of occurring,

$$G(q_s, P) = q_s(P) \times P. \tag{5}$$

The distribution for White Sands exhibited a well defined peak, G_{max}, at q_s = 0.017 kg m^{-1} s^{-1} (Figure 4), resulting in a predicted value for the dune-forming wind of u_{*f} = 0.39 m/s. This value will be used for calculations of sediment mobility in this paper. This approach is analogous to models of river evolution, where the complex hydrograph is reduced to (1) a constant "formative" shear stress and (2) an intermittency factor describing the fraction of time that the formative stress is active. [e.g., *Paola et al.*, 1992]. For White Sands, winds equal to or greater than the formative wind occur approximately 3% of the time.

4. Results

4.1. Bulk Downwind Trends and Sorting Over Dunes

[16] As discussed above, samples were taken in dune stoss, crest and lee positions from 0 km to 5.7 km, while only dune crests were sampled further downwind. Data show a general decrease in dispersion with distance, indicating that grains become better sorted downwind (Figure 5). A power law fit shows that the residuals are nonrandomly distributed; dune crest samples systematically plot below the trend, while stoss samples plot above the trend. (Lee samples are intermediate and do not depart significantly from the trend.) Dune crests are thus significantly better sorted than lower stoss positions, and this difference accounts for 25% of the total sample variance (Figure 5). Stronger sorting on dune crests has been observed in several other studies [*Barndorff-Nielsen et al.*, 1982; *McLaren and Bowles*, 1985; *Lancaster*, 1995; *Pye and Tsoar*, 2009], and has been attributed to both an inability for large grains to be transported up dune faces, and/or the mixing of coarse-grained, avalanche slip-face deposits with saltating grains that occurs in dune troughs but not on crests [*Pye and Tsoar*, 2009]. Although intradune sorting is fascinating, it obscures the overall downwind patterns of sorting and abrasion we wish to study and so will not be considered further. To correct for this effect, we consider only samples taken from dune crests for the rest of this paper.

[17] Interestingly, there is little to no change in the median grain diameter of dune crest sediments over the 9 km transect (Figure 6a). The most significant trends observed were increased sorting (decreased dispersion; Figure 6c) and decreased average elongation (Figure 6d) downwind.

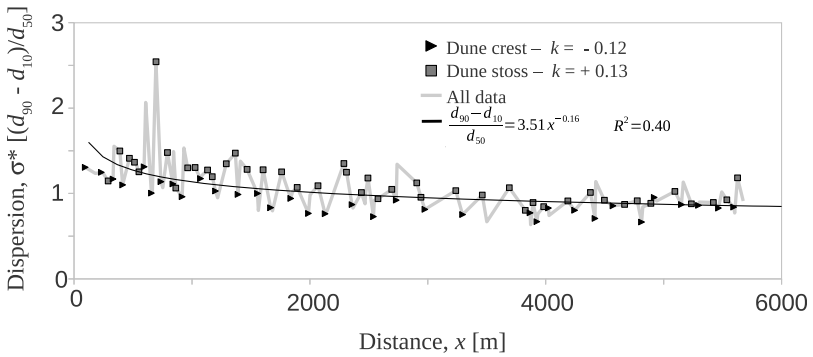

Figure 5. Normalized dispersion, a proxy for sediment sorting, along the first ~5700 m of the transect. Gray line shows all surface samples taken over this distance, while markers indicate locations of dune crest and stoss samples, indicated in legend. Black line shows best fit regression to data, where x has units of meters. Note that crests are systematically less disperse (more sorted) than stoss samples. Residuals (k, dimensionless) for crest and stoss samples show negative and positive dispersion bias, respectively.

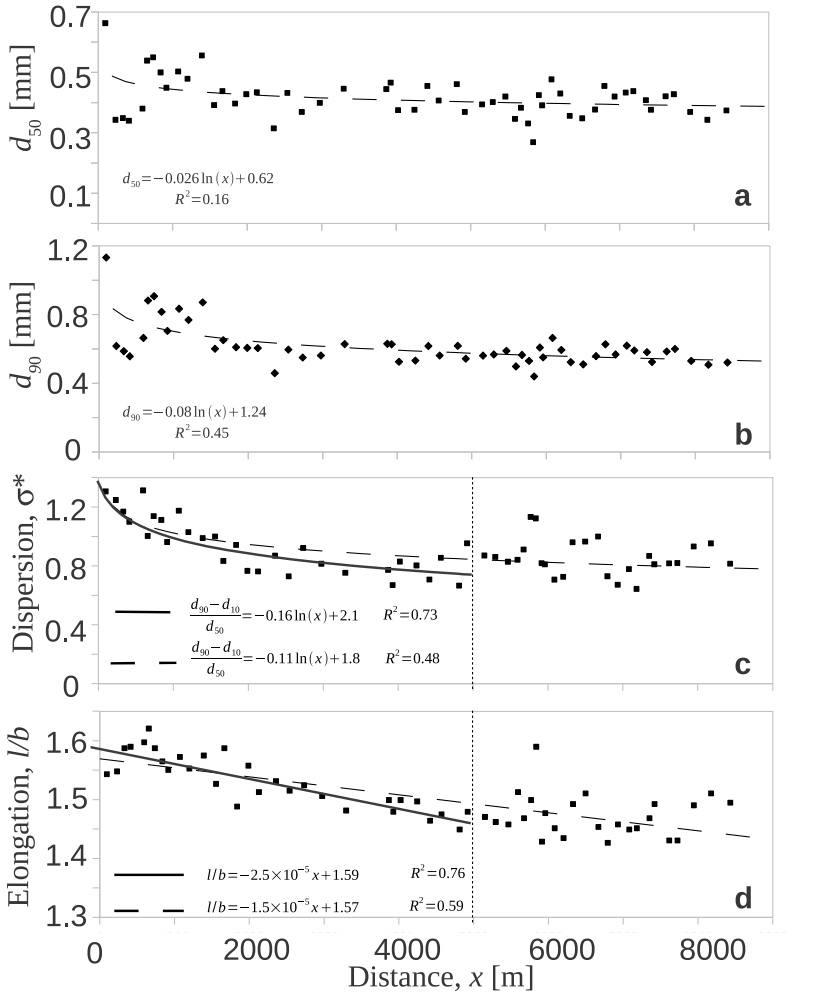

Figure 6. Bulk grain size and shape data from dune crests sampled along the transect, with best fit regression (dotted lines). (a) Diameter d_{50} does not change significantly downwind, as noted by poor fit of regression equation. (b) Diameter d_{90}, (c) dispersion, and (d) elongation downwind. Note rapid decline in size dispersion over the first few kilometers and leveling off beyond 5 km. Elongation decreases more slowly but also appears to level off by 5 km. Arbitrarily separating the data at 5 km, we obtain better fits to elongation and dispersion data (solid lines). See text for details.

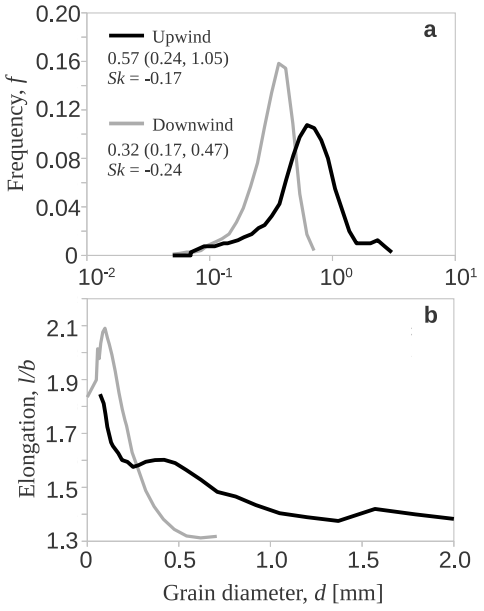

Figure 7. Representative (a) grain size distribution and (b) elongation data for an upwind (x = 2 km, black line) and downwind (x = 8 km, gray line) dune crest sample. If GSDs are represented as lognormal, they are negatively skewed (*Sk*) toward the fine fraction, and skewness increases downwind. Legend in Figure 7a denotes grain size, d_{50} (d_{10}, d_{90}).

Measurements show that most of the change in dispersion is due to a decrease in the d_{90} (Figure 6b), that is, loss of coarse grains from the system. Dispersion decreases rapidly over the first few kilometers, then levels off to a more-or-less constant value. Elongation shows a gradual but persistent decrease over the same distance, and also appears to level off further down the dune field (Figure 6). (Note that elongation values presented in Figure 6 represent a volumetric average for each sample, and thus are disproportionately affected by the behavior of larger grains.) The apparent saturation in dispersion and elongation at distances greater than 5 km indicates that sorting and/or abrasion processes act principally in the upwind section of the dune field. Arbitrarily separating the data at 5 km, we obtain significantly better regression fits over the interval 0–5 km compared to fitted data over the entire range (Figures 6c and 6d). Overall, the data indicate that grains become both better sorted and more equant as they are transported, with most of that change occurring over the first 5 km downwind of the sediment source. The net decrease in dispersion is approximately 40%, while change in the average elongation is more modest at about 10%.

4.2. Grain Size and Shape Distributions

[18] More insight into the processes of sorting and abrasion may be gained by analyzing individual grain size distributions (GSDs), and their corresponding shapes. Both exhibit obvious changes from the upwind to downwind margins of the dune field (Figure 7). Grain sizes are typically reported or assumed as lognormal distributions [*Spencer*, 1963; *Rogers and Schubert*, 1963]. If White Sands data are treated this way, GSDs are systematically lognormal skewed toward the fine fraction (Figure 7a). Despite the downwind decrease in overall dispersion reported above, distributions become slightly more finely skewed (less symmetric) with distance. An alternative representation of GSDs is to plot them in log-log scale, a method introduced by *Bagnold* [1941] who suggested that GSDs are better described by log-hyperbolic functions (see discussion by *Barndorff-Nielsen* [1977] and *Pye and Tsoar* [2009]). Using this method, he found that coarse and fine tails exhibit independent, power law relationships between grain size and frequency (Figures 8a and 8b). *Bagnold* [1941] observed that the (negative) slope of the coarse tail, c, is invariably larger in magnitude than the slope of the fine tail, s; in effect, the distributions are skewed toward the fine fraction. White Sands data appear to be well characterized by log-hyperbolic relationships, allowing a convenient representation of the GSDs in terms of the slopes s and c (Figures 8a and 8b). It is clear that GSDs tend toward a constant shape at distances larger than 5 km (Figure 8b).

[19] We fit separate power laws to the fine and coarse tails of all GSDs along the transect, excluding the mode and the three points on either side of it in order to avoid curvature effects at the peak of the distribution. Plots of slope values along the transect show that the magnitude of c increases toward a constant value at distances beyond 5 km, while s does not vary systematically across the transect (Figure 9, top). Fluctuations in c and s (Figure 9, top) likely represent a combination of real high-frequency variations in grain sorting, and also some noise introduced from fitting slopes to a small number of points. The asymptotic value for c in White Sands is close to the apparent limiting value c = 9 observed by *Bagnold* [1941] for wind-blown sediment, while s falls within his commonly observed range of $2 \leq s \leq 3$ (Figures 8a; 8b; and 9, top). The remarkable commonality of s and c among wind-blown sediments [see also *Barndorff-Nielsen*, 1977] in different deserts is a point we will return to later.

[20] A look at elongation data for individual size classes is revealing. Coarse grains are less elongate than fine grains for all samples analyzed, including the sediment source (Figure 7b). This disparity increases downwind; in other words, large grains become more equant while finer grains become more prolate (or the proportion of prolate finer grains increases; see Figures 7 and 8). For example, l/b values for the particle size class d = 0.54 mm decrease from 1.6 to 1.3, while l/b values for class d = 0.19 mm increase from 1.7 to 2.0 (Figure 9, bottom). As with grain size data, elongation values for all particle sizes stabilize beyond a distance of 5 km downwind (Figures 8d and 9, bottom); plots of elongation against particle diameter fall on top of each other beyond 5 km (Figure 8d). Microscopic images of grains support and inform size and shape metrics. It is clear that source grains are large and exhibit complex bladelike and rodlike patterns that reflect the structure of crystalline gypsum (Figure 10a). Just several hundred meters downwind, these (likely fragile) structures cannot be found; grains are generally smaller and take on a rounder appearance and range from prolate to equant in shape (Figure 10b). Toward the downwind end of the dune field, there are no prolate grains to be found among the coarse population of sediment (Figure 10d). Images qualitatively suggest that both breaking and chipping of grains occur, because bladed

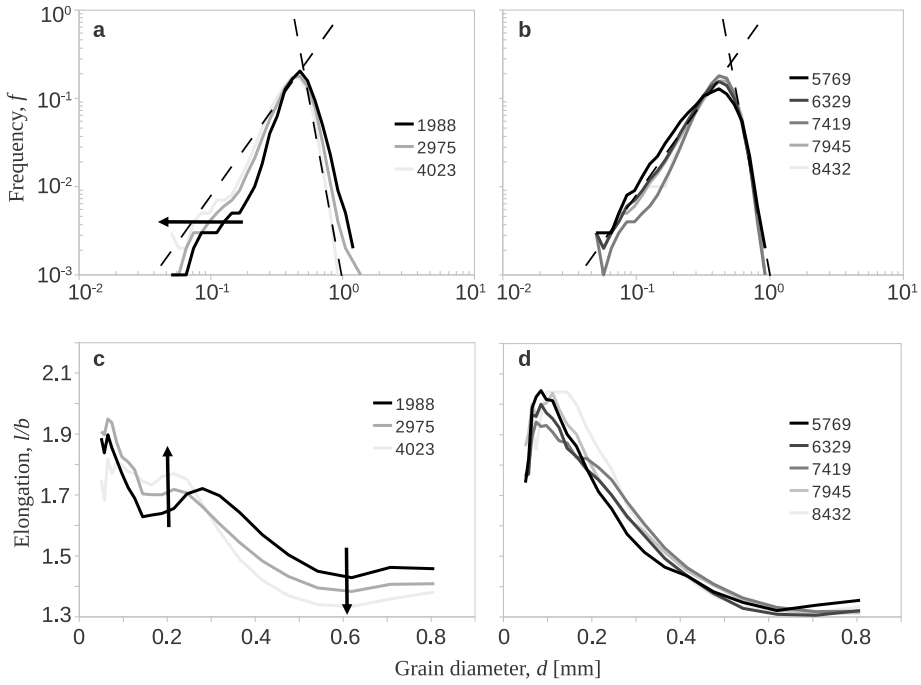

Figure 8. Grain size distributions in log-log plots, and elongation data, shown across the transect. Legends indicate position along the transect in meters. Distributions appear to be reasonably described by log-hyperbolic functions, where the fine and coarse limbs have slopes denoted by *s* and *c*, respectively. (a) GSDs show that *c* increases over the first few kilometers of the dune field and suggest enrichment of a fine-grained fraction (indicated by arrow). Dashed lines indicate *Bagnold*'s [1941] limits for *s* and *c* associated with a strong wind. (b) Beyond 5 km, GSDs become approximately stationary around the limiting values of *s* and *c*. (c) Large grains become less elongate and small grains become more elongate (indicated by arrows), moving downwind from 2 km to 4 km. (d) Beyond 5 km, elongation ceases to change and abrasion is likely less efficient.

structures disappear (breaking) while the edges of grains appear to get more round (chipping) downwind. Changes in elongation and size are not monotonic; a few samples in the vicinity of 5–6 km show anomalously large, prolate and angular grains (Figure 10c) that could not have traveled far in transport and therefore might have a local source. These samples, however, are rare enough that they do not disrupt downwind trends.

5. Discussion

[21] It is clear that there are systematic trends in grain size and elongation moving downwind from the sediment source, but also that size and elongation distributions become approximately stationary beyond a distance of 5–6 km. Assuming that all sediments originate from the same source at $x = 0$ km, these changes must be the result of sorting and/or abrasion of particles. Abrasion is certainly expected because gypsum is so easily erodible [see *Pye and Tsoar*, 2009], however, the effects of sorting must be quantified before one can attribute changes in size and shape to abrasion. The decrease in bulk elongation with downwind distance (Figure 6) would suggest that the shape of particles is modified by abrasion, while decrease in dispersion could be attributed to sorting. However, this simple interpretation neglects the possibility that grains may also be sorted by shape during transport. Although studies of "shape sorting" are not all in agreement, there is some evidence that spherical, rounded sand grains may be more easily transported by wind [*Willetts et al.*, 1982; *Mazzullo et al.*, 1986; *Pye and Tsoar*, 2009]. Thus, at least some of the downwind reduction in elongation could be due to shape-selective sorting rather than a real modification of individual particle shape by abrasion. In order to separate sorting from abrasion effects, two approaches are taken: (1) we assess the relative mobility of different particle sizes to determine what sorting would be expected based on size-selective transport alone, and (2) we show that some elongation patterns are statistically independent of sorting patterns, and therefore can likely be attributed to abrasion.

5.1. Modes of Transport and Sorting

[22] In his pioneering study of grain-size sorting patterns in a wind tunnel, *Bagnold* [1941] suggested that "the grading of the total sand removed from a bed of regular sand and set in motion by a wind is not itself regular, but it can be treated as a mixture of three regular constituents which appear to correspond to the three modes of transportation—saltation, surface creep, and suspension." In other words, Bagnold was stating that particles that move by different modes of transport will behave independently of one

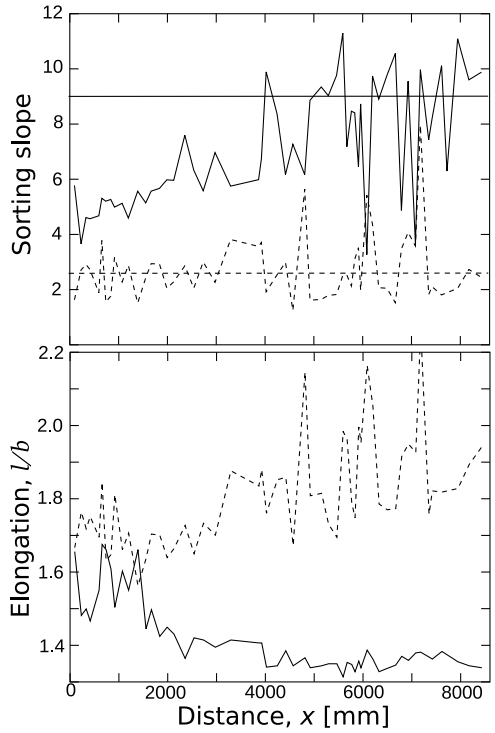

Figure 9. (top) Magnitude of sorting slopes for coarse (*c*, denoted by solid line) and fine (*s*, dashed line) limbs of the GSD down the transect. Note that the coarse limb becomes larger (better sorted) downwind, but saturates around *Bagnold*'s [1941] limiting value of about $c = 9$ (solid line) beyond a distance of 5 km. Fine limb fluctuates around a value of $s = 2.5$ (dashed line). (bottom) Elongation for representative grain size classes: solid line represents grains in saltation ($d = 0.54$ mm), and dashed line is a representative suspension size class ($d = 0.19$ mm). Elongation trend for saltating grains is not strongly coupled to sorting, while elongation fluctuations for suspended grains strongly covary with fluctuations in sorting (see text).

another. This idea is deeply connected to his observation that the slopes *s* and *c* in a GSD vary independently of one another. It is thus critical to define the style of transport for different particle diameters. For purposes of this paper, we define the three modes simply (for more detail see, e.g., *Bagnold* [1941], *Anderson and Haff* [1988], *Fryberger et al.* [1992], *Nalpanis et al.* [1993], *Nishimura and Hunt* [2000], and *Pye and Tsoar* [2009]): (1) suspension describes grains that are held aloft by the turbulent flow and have only infrequent contact with the bed; (2) saltation refers to grains that travel in ballistic trajectories in between frequent, energetic collisions with the bed; and (3) creep describes grains that are too heavy to be moved directly by the wind, but move slowly along the bed due to the combined forces of aerodynamics and collisions from saltating grains. Abrasion is expected to be most significant for saltating grains, and negligible for suspended sediment due to infrequent and less energetic collisions with the bed.

[23] Following *Nishimura and Hunt* [2000], we define the range of grains that are in saltation using their wind tunnel derived estimate, $u_{*c} \leq u_{*f} \leq 1.5u_{*c}$. Grains in suspension satisfy two constraints [*Nishimura and Hunt*, 2000; *Jerolmack et al.*, 2006]: (1) $u_{*f} \geq 1.5u_{*c}$ and (2) $u_{*f}/w_s \geq 3$, where w_s is the terminal settling velocity of particles and was estimated using the expression of *Ferguson and Church* [2004]. Based on our calculations (Figure 11a), the first constraint is the more restrictive of the two and may thus serve as a general guide for delineating the suspension population. Grains travel in creep when transport conditions are in the range $0.7u_{*c} \leq u_{*f} < u_{*c}$ [*Bagnold*, 1941; *Nishimura and Hunt*, 2000; *Jerolmack et al.*, 2006]. Calculations for White Sands make the following predictions for approximate grain size ranges associated with each mode of transport: suspension for $d < 0.25$ mm, saltation for $0.25 \text{ mm} < d < 0.65$ mm, and creep for $0.65 \text{ mm} < d < 1.30$ mm (Figure 11a). Note that the median grain size for the dune field, $d_{50} = 0.40$ mm, falls right in the middle of the expected saltation population range, providing support for the idea that dune sands represent the population of grains that are frequently saltated but rarely suspended in a given wind regime. Moreover, the average $d_{10} = 0.22$ mm and the average $d_{90} = 0.58$ mm, when computed from all surface samples at distances beyond $x = 2$ km. These values are remarkably close to the computed lower and upper grain sizes, respectively, of the expected saltation population. Thus, the dune-forming wind determines not only the peak of the grain size distribution but also the width of this distribution; the range of grains in saltation corresponds approximately to 2σ, where σ is the standard deviation of the GSD.

[24] Grains larger than 1.3 mm should rarely be transported, and thus, we expect not to see grains of this size beyond some small distance from the source, consistent with

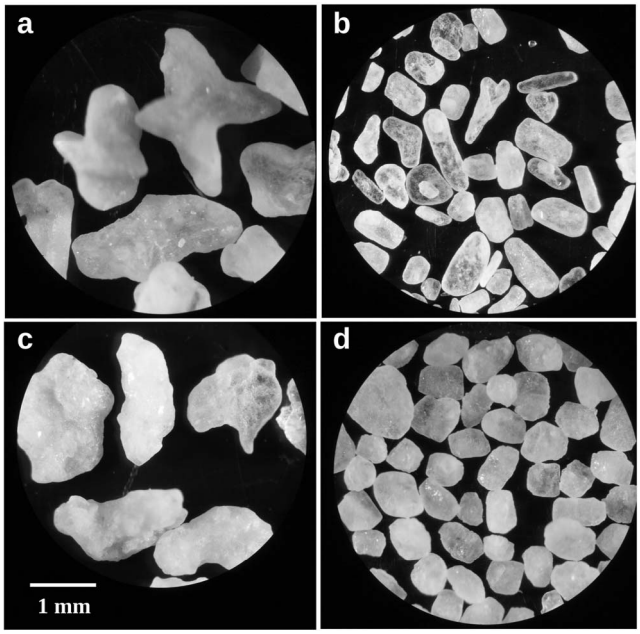

Figure 10. Microscopic images of dune crest samples downwind. Scale applies to all images. (a) Sample taken from the crest of a small "dome" dune, at $x = 94$ m. (b) Image at $x = 331$ m. (c) Rare sample of large, prolate, angular grains found at $x = 5700$ m, indicating a nearby (though not significant) sediment source. (d) More equant, blocky grains representative of the downwind saltation population ($x = 7485$ m).

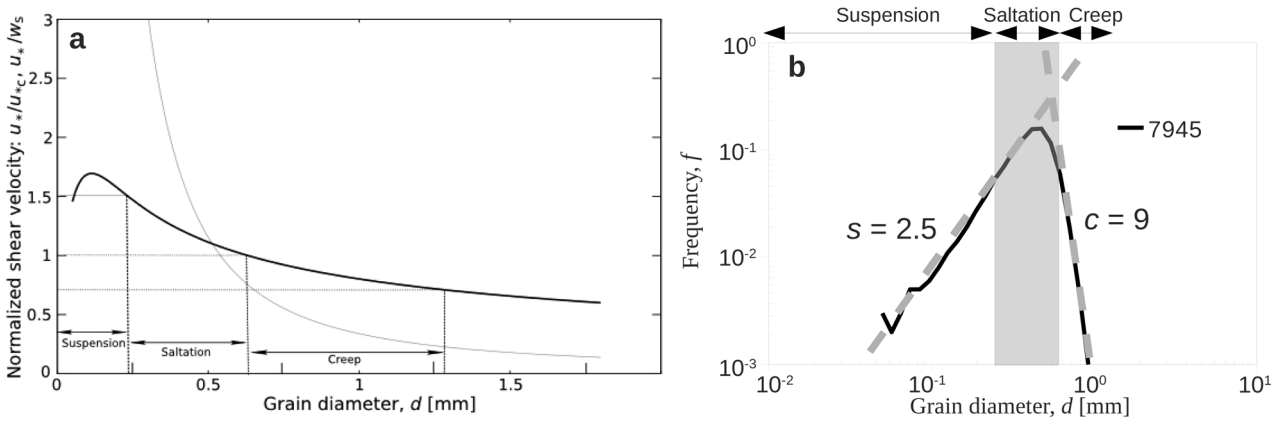

Figure 11. Estimates of grain mobility under the dune-forming wind, u_{*f} = 0.39 m/s. (a) Plot of shear velocity normalized in terms of critical shear velocity (black line) and settling velocity (gray line). Predicted modes of transport estimated using methods in text. Grains larger than d = 1.3 mm are not expected to be moved at all, while grains smaller than d = 0.25 mm should move primarily by suspension. Grains in between move by saltation and/or creep. (b) A typical downwind grain size distribution (x = 7945 m) that is "mature," showing Bagnold's limiting sorting slopes. The gray box indicates particle sizes predicted to travel in saltation under the dune-forming wind; particles to the left travel in suspension, while those to the right travel in creep.

observations showing that d_{90} never exceeds this value beyond the sediment source (Figure 6b). Another expectation is that grains in creep should not be transported as far as saltating grains, because they travel slowly by rolling along the ground [*Bagnold*, 1941; *Lancaster*, 1995]. Indeed, data show that d_{90} decreases from 0 km to 2 km from the source before leveling out around d_{90} = 0.58 mm, close to the predicted lower range of creep (Figure 6d). Results imply that most grains traveling primarily in creep have not penetrated beyond 2 km from the source, although a small fraction is present further downwind (Figure 11). Grains smaller than ~0.25 mm travel in suspension under the dominant wind (Figure 11). *Bagnold* [1941] observed that suspended grains may settle over the dune field as a more-or-less uniform drape as strong winds subside, leaving little or no spatial sorting trend. Thus, the slope of the coarse limb of the GSD (c) is expected to increase downwind, while the slope of the fine limb (s) may be expected not to vary. This is exactly the trend observed in White Sands data (Figure 9, top).

5.2. Sorting Limits

[25] In experiments and natural observations, *Bagnold* [1941] was unable to find wind-blown sediments having a coarse tail slope c greater than 9 [*Barndorff-Nielsen*, 1977], and indeed White Sands GSDs stabilize at a value c = 9 at a distance of 5 km. Our relatively constant value for the fine tail of s = 2.5 is consistent with *Bagnold*'s [1941] measured sorting for experiments undergoing a "strong wind" (strength not specified, but significantly above entrainment threshold). The limiting behavior of sorting observed by *Bagnold* [1941] and supported by our data (Figure 11a) does not yet have a theoretical underpinning [*Barndorff-Nielsen*, 1977], but our analysis solidifies some of Bagnold's hypotheses regarding the relation between modes of transport and the shape of a GSD. Moving downwind in our transect, the asymptotic scaling of s and c indicates that downwind sediments are "mature" and can be sorted no further. When we project the expected ranges of suspension, saltation and creep onto a typical mature (downwind) GSD, we can see how each mode of transport imparts its signature on the shape of the GSD. Suspended grains compose the fine-grained part of the distribution that is described by positive slope, s = 2.5; saltating grains delineate the curved hump of the GSD that connects the two limbs; and creeping grains are represented by the negative coarse-grained slope, c = 9 (Figure 11b).

[26] The conclusions we can draw are that grains traveling in suspension are not strongly sorted downwind, while coarser grains appear to exhibit size-selective transport downwind until only grains traveling mostly in saltation under the dominant wind are left, at which point sorting ceases to evolve. Thus, all of the first-order trends regarding grain size distributions appear to be explained by size-selective sorting under a single, dune-forming wind, without considering abrasion at all.

5.3. Elongation and Abrasion

[27] It is important to remember that particle diameter is measured using the b axis (i.e., $b \approx d$), which means that a decrease in elongation (l/b) may occur without a significant change in particle diameter d. In such a scenario, decreasing elongation means decreasing l. It appears likely that this is what occurs at White Sands. We turn our attention to aspects of particle elongation that may not be ascribed to size- or shape-selective sorting. Although dispersion and elongation both decrease downwind together, they do not do so at the same rate. Dispersion decreases rapidly in the first 2 km, an effect we attributed to size-selective sorting, while elongation decreases more slowly but persistently up to about 5 km (Figure 6). A correlation analysis shows that only 22% of the variance in elongation may be explained by

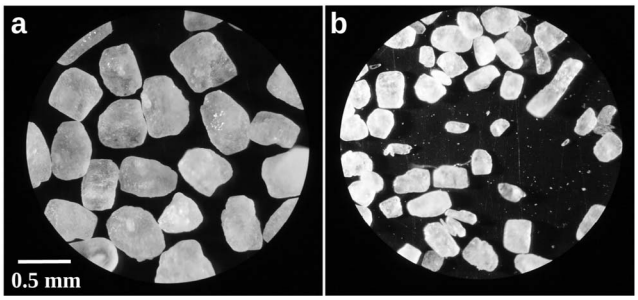

Figure 12. Dune crest at x = 7485 m (same as Figure 10d) sieved into fractions (a) greater than and (b) less than d = 0.25 mm. Note finer grains are more elongate and angular. Scale applies to both images.

dispersion, so some other factor must be sought. According to our transport calculations, we expect that elongation for particles larger than 0.25 mm should decrease due to saltation abrasion, while elongation for smaller particles should remain constant or increase downwind because the particles are suspended. Figure 7b provides qualitative support for this idea, as all grains larger than d = 0.25 mm become less elongate downwind, while grains smaller than that become more elongate. Separating grains into two populations using a 0.25 mm sieve, it is apparent that larger grains are more equant and rounded, while smaller grains are more elongate and angular (Figure 12). We hypothesize that grains smaller than 0.25 mm are abrasion products, resulting from spallation and breaking of saltating grains. Particles with b = 0.1–0.2 mm are prolate, and have a shape and size consistent with breaking of larger grains. The smaller particles, which appear as flecks in the images, are likely either spallation products resulting from chipping of corners by abrasion or shattered byproducts of breaking (Figure 12). That elongation for suspended grains actually increases downwind (Figures 7b; 8b; 8c; and 9, bottom) suggests that either individual grains are becoming more elongate as they travel, or that there is an enrichment of elongate grains downwind.

[28] We quantitatively examine the downwind evolution of two representative grain sizes, a saltating size class with d = 0.54 mm and a suspended size class with d = 0.19 mm, in terms of elongation (Figure 9) and the sorting slopes s and c. Elongation of d = 0.54 mm decreases significantly with distance downwind, while sorting of coarse grains (c) increases downwind (Figure 9). We remove these trends to examine whether fluctuations in sorting covary with fluctuations in elongation. Regression analysis reveals that only 12% of the variance in elongation may be explained by sorting. In other words, neither the trend nor fluctuations around the trend of sorting can account for the majority of the variance in elongation. This provides strong evidence that individual grains are actually becoming more equant downwind by saltation abrasion. For d = 0.19 mm grains, a different behavior is expected due to a different mode of transport. A casual comparison of downwind evolution for elongation (l/b) and fine-grained sorting (s) shows striking similarity in the covariance of these parameters (Figure 9). After detrending the two data series, regression analysis shows that 71% of the variance in elongation for d = 0.19 mm can be accounted for by sorting alone. Our interpretation is that the overall increase in elongation downwind for small grain sizes has to do with enrichment of abrasion products from saltation, while fluctuations in elongation are strongly related to spatial variations in sorting. Thus, shape change of saltating particles can be attributed to abrasion, while shape variations in suspended particles result mostly from sorting and not abrasion.

5.4. Abrasion Limits and Shape Effects

[29] The stabilization of elongation at distances greater than 5 km (Figures 8c and 8d) means that abrasion is somehow no longer able to affect grain shape, and suggests a possible control of shape itself on the abrasion process. Experiments discussed earlier that used clay "pebbles" to study particle abrasion also found a limiting, noncircular shape, exhibiting deviations in curvature that represented the limited effectiveness of spallation in chipping off corners [*Durian et al.*, 2006; 2007]. *Kuenen* [1960] reported that abrasion rate of quartz sand decreased with decreasing angularity of grains. Taken together, these studies suggest that abrasion occurs most readily when protrusions on grains are present and that, as these protrusions are removed, the effectiveness of abrasion diminishes. The sediment source at White Sands clearly contains particle shapes that are fragile and would break apart upon saltation (Figure 10). The rapid decrease in elongation of the saltating grain fraction over the first 2 km (Figure 9, bottom) likely results from breaking of unstable protrusions on grains. We would expect an enrichment of prolate, possibly angular particles having a maximum size corresponding to the reduction in elongation of coarser grains. For a particle of d = 0.8 mm (near the upper limit of grains found in appreciable quantities across the dune field) with a reduction in elongation of 0.3, this translates to a maximum abrasion product of d = 0.24 mm; for the median grain size d = 0.4 mm, the expected maximum abrasion product would be d = 0.12 mm. The former corresponds to the upper limit of suspended sediments, while the latter matches nicely the peak in elongation seen in Figure 8d. Thus it is plausible that much of the population of suspended sediment at White Sands is actually the product of saltation abrasion of larger particles, and that the increased elongation observed downwind for these particles is due to accumulation of abrasion products.

[30] We note the upper limit on abrasion products at White Sands is significantly larger than the silt and dust sizes observed for quartz grains [*Bullard et al.*, 2004, 2007], and this is because breaking of fragile gypsum structures produces larger particles than spallation alone. All grains larger than d = 0.25 mm become more equant downwind (Figures 8c and 8d), and the rate of decrease in elongation appears to increase with particle size. The result is that, at saturation, the largest saltating grains are the least elongate, while elongation increases with decreasing grain size down to d = 0.1 mm (Figure 8d). Thus, the curves in Figure 8d represent the stable limiting shape for grains of a given diameter. We cannot yet predict what controls abrasion rates for different particles, but the stable curves (Figure 8d) indicate that it is a combination of collision energy and grain shape. Larger grains have more collision energy, and can thus produce more equant particles. Smaller saltating grains collide with less vigor and thus are less efficient at removing protruding edges. Grains in suspension reflect the shape

imparted on them when liberated in the collision process, and do not experience significant alteration during transport because of their infrequent and low-energy collisions with the bed. The "hinge-point" between grains that abrade and the products of those grains (Figure 7b) occurs at the boundary of saltation and suspension under the dune-forming wind condition, corresponding to approximately $d = 0.25$ mm for White Sands. Thus, there appears to be a limiting particle shape for a given collision energy. It is possible that abrasion continues for these grains, but it must be at a reduced rate.

5.5. Threshold Sand Sea Hypothesis and Reconstructing Winds

[31] That a single representative value for wind velocity, derived using a single grain size, is able to predict the transport and sorting dynamics of the entire grain population is remarkable. The result supports the "threshold sand sea" hypothesis [see *Jerolmack and Brzinski*, 2010] which states that the predominant grain size in a sand sea represents particles that are not too far above the threshold for entrainment under the dominant wind. *Jerolmack and Brzinski* [2010] examined four deserts and found that the dimensionless (Shields) formative stress, $\tau_{*_f} = \rho u_{*f}^2/[(\rho_s - \rho)gd]$, covers the range $1.5\tau_{*_c} \leq \tau_{*_f} \leq 2\tau_{*_c}$, such that the formative stress is within a factor of two of the critical stress τ_{*c} required for entrainment. This is a logical consequence of the notion that dunes are composed of grains traveling principally in saltation (beginning from *Bagnold* [1941]). The upper limit for formative wind stress should approximately equal *Nishimura and Hunt*'s [2000] upper limit for saltation, $u_{*_f} \leq 1.5u_{*_c}$, or $\tau_{*_f} \leq u_{*_f}^2/u_{*_c}^2 \leq 2.25\tau_{*_c}$. The lower limit, of course, is the limit for entrainment. The expected "theoretical" range for formative wind stress in deserts is thus

$$u_{*_c} \leq u_{*_f} \leq 1.5u_{*_c} \tag{6a}$$

or

$$\tau_{*_c} \leq \tau_{*_f} \leq 2.25\tau_{*_c}. \tag{6b}$$

Because grains must be frequently saltated in order to move a significant distance away from the source, but rarely suspended such that they remain within a dune field, the modal value for the formative wind is likely somewhere between the limits. We might tentatively predict that sand seas cluster around the condition

$$u_{*_f} \approx 1.25u_{*_c} \tag{7a}$$

or

$$\tau_{*_f} \approx 1.6\tau_{*_c}. \tag{7b}$$

A compilation of formative winds for dune fields around the world, following the procedures outlined here, could test this idea.

[32] The narrow range of formative winds associated with the presence of sand dunes also allows one to place tight constraints on paleowinds from grain size alone. Using either (6) or, if demonstrated by data, the more precise (7), it is simple to back-calculate the magnitude of the dune-forming wind using a measured d_{50} of preserved dune sediments and the threshold entrainment expression (2). Additional verification could use the entire grain-size population of a sample, as it appears that the d_{10} and d_{90} of surface sediments correspond with the upper and lower limits for saltation, respectively, defined in (6).

6. Conclusions

[33] Despite the soft nature of gypsum, size-selective sorting by sediment transport, rather than abrasion, is still the dominant process controlling downwind changes in grain size at White Sands. This sorting can be succinctly characterized using a representative dune-forming wind, which is the wind velocity that produces the largest annual sand flux for the median grain size. This formative wind may be used to classify the dominant mode of transport for all grain sizes. Results from White Sands show that most grains in creep travel only a few kilometers from the source, while grains in saltation make up the dominant population of the dune field, and grains in suspension are present everywhere in the bed in small concentration. We refine the threshold sand sea hypothesis [*Jerolmack and Brzinski*, 2010] here, to state that the median grain size of sand seas represents the size class that lies in the middle of the range of saltating particles under the dune-forming wind. In addition, it appears that the width of the grain size distribution, as measured by d_{90}–d_{10}, represents the total range of grains in saltation under this dominant wind. If verified by additional studies in other deserts, these findings provide a useful simplification for predicting grain mobility and sorting in eolian environments, and also for reconstructing paleowinds using the grain size of preserved dune sediments. Downwind grain-size sorting at White Sands saturates when the distribution reaches the empirically determined limits observed by *Bagnold* [1941]. Although an explanation for the numerical values of these limits remains elusive, we can break the curve into three parts which are each related to a mode of transport – suspension, saltation and creep.

[34] Despite the prevalence of sorting, we were still able to detect the signature of abrasion in grain shape. Measurements of elongation indicate that abrasion acts preferentially according to size. Grains in saltation wore down to become more equant, with the degree of abrasion increasing with grain size. Elongation for suspended grains increased downwind, likely because of an enrichment of these prolate grains. A large fraction of suspended sediments at White Sands are likely the breaking and spallation products resulting from abrasion of saltating particles. Due to the particular character of crystalline gypsum, sand particles appear to undergo some breakage during transport, and thus abrasion products may reach fine to medium sand in size. This is unlikely to occur in quartz-rich sand seas, where abrasion products are generally limited to spalled chips in the dust- to silt-size range [e.g., *Bullard et al.*, 2004, 2007]. In addition, harder quartz grains mean that detecting abrasion would require a study over much greater distances. Nonetheless, it should be generally true that grains in suspension under the formative wind will not experience significant abrasion, while saltating grains will. Another potentially generalizable result is that abraded grains reach some asymptotic shape that is not circular [*Durian et al.*, 2006]. At White Sands this corresponds to a threshold value for elongation, below

which grains cannot abrade (or at least, abrade much more slowly) under the current wind regime. It appears that abrasion rate depends not only on collision energy (and hence grain size) but also on the shape of the grain, which determines its susceptibility to breaking or spallation. Thus, each size class of saltating particles in a desert (and river) environment should have a limiting shape, which is determined by its particular combination of mineralogy, flow regime, and grain size distribution. Mature grains at White Sands reach a limiting size and shape distribution as a combination of sorting and abrasion.

[35] It is clear that we can only extrapolate so far, however, from our field measurements without a firm theoretical and experimental basis. The conventional wisdom is that abrasion significantly affects grain size distributions in eolian sand seas but not in alluvial rivers; however, this idea is challenged by data and calculations suggesting a dynamic similarity between these two environments [*Jerolmack and Brzinski*, 2010]. Properly scaled experiments on particle collision are needed that isolate the effects of both energy transfer and grain shape on abrasion, for a range of mineralogies. A theoretical approach should combine the shape control modeled in corner cutting simulations [*Durian et al.*, 2007; *Krapivsky and Redner*, 2007], with an energetics model for grain collisions [e.g., *Anderson*, 1986]. Such a generalized approach will provide a unified framework for sorting out abrasion in deserts and rivers.

[36] **Acknowledgments.** Research was supported by the Department of Earth and Environmental Science at UPenn for the GEOL305 class trips of 2009 and 2010 and also by the National Science Foundation through agreement EAR-0846233 to D.J.J. We thank Dajana Jurk, Anastasia Piliouras, Melissa Retkwa, Felix Lim, Ryan Ewing, and the rest of the field team for their assistance in collecting and analyzing these data. We are especially grateful to David Bustos of the National Park Service (NPS) for facilitating this study. LiDAR data were kindly supplied by Gary Kocurek, and were funded by a grant from NPS as part of the Chihuahuan Desert Network Inventory and Monitoring Program. Ideas and suggestions by Theodore Brzinski and Douglas Durian were helpful in developing this manuscript.

References

Anderson, R. (1986), Erosion profiles due to particles entrained by wind - application of an eolian sediment-transport model, *Geol. Soc. Am. Bull.*, *97*(10), 1270–1278, doi:10.1130/0016-7606(1986)97<1270:EPDTPE>2.0.CO;2.

Anderson, R., and P. Haff (1988), Simulation of eolian saltation, *Science*, *241*(4867), 820–823, doi:10.1126/science.241.4867.820.

Bagnold, R. (1941), *The Physics of Blown Sand and Desert Dunes*, Methuen, London.

Barndorff-Nielsen, O. (1977), Exponentially decreasing distributions for the logarithm of particle size, *Proc. R. Soc. London, Ser. A*, *353*(1674), 401–419.

Barndorff-Nielsen, O., K. Dalsgaard, C. Halgreen, H. Kuhlman, J. Møller, and G. Schou (1982), Variation in particle size distribution over a small dune, *Sedimentology*, *29*(1), 53–65, doi:10.1111/j.1365-3091.1982.tb01708.x.

Bullard, J., G. McTainsh, and C. Pudmenzky (2004), Aeolian abrasion and modes of fine particle production from natural red dune sands: An experimental study, *Sedimentology*, *51*(5), 1103–1125, doi:10.1111/j.1365-3091.2004.00662.x.

Bullard, J., G. McTainsh, and C. Pudmenzky (2007), Factors affecting the nature and rate of dust production from natural dune sands, *Sedimentology*, *54*(1), 169–182, doi:10.1111/j.1365-3091.2006.00827.x.

Crouvi, O., R. Amit, Y. Enzel, N. Porat, and A. Sandler (2008), Sand dunes as a major proximal dust source for late Pleistocene loess in the Negev Desert, Israel, *Quat. Res.*, *70*(2), 275–282, doi:10.1016/j.yqres.2008.04.011.

Crouvi, O., R. Amit, Y. Enzel, and A. Gillespie (2010), Active sand seas and the formation of desert loess, *Quat. Sci. Rev.*, *29*(17–18), 2087–2098, doi:10.1016/j.quascirev.2010.04.026.

Durian, D., H. Bideaud, P. Duringer, A. Schröder, F. Thalmann, and C. Marques (2006), What is in a pebble shape?, *Phys. Rev. Lett.*, *97*(2), doi:10.1103/PhysRevLett.97.028001.

Durian, D., H. Bideaud, P. Duringer, A. Schröder, and C. Marques (2007), Shape and erosion of pebbles, *Phys. Rev. E*, *75*(2), doi:10.1103/PhysRevE.75.021301.

Ewing, R., and G. Kocurek (2010a), Aeolian dune interactions and dune-field pattern formation: White Sands Dune Field, New Mexico, *Sedimentology*, *57*(5), 1199–1219, doi:10.1111/j.1365-3091.2009.01143.x.

Ewing, R., and G. Kocurek (2010b), Aeolian dune-field pattern boundary conditions, *Geomorphology*, *114*(3), 175–187, doi:10.1016/j.geomorph.2009.06.015.

Ewing, R., G. Kocurek, and L. Lake (2006), Pattern analysis of dune-field parameters, *Earth Surf. Processes Landforms*, *31*(9), 1176–1191, doi:10.1002/esp.1312.

Ferguson, R., and M. Church (2004), A simple universal equation for grain settling velocity, *J. Sediment. Res.*, *74*(6), 933–937, doi:10.1306/051204740933.

Fryberger, S., P. Hesp, and K. Hastings (1992), Aeolian granule ripple deposits, Namibia, *Sedimentology*, *39*(2), 319–331, doi:10.1111/j.1365-3091.1992.tb01041.x.

Goudie, A. S., and A. Watson (1981), The shape of desert sand dune grains, *J. Arid Environ.*, *10*, 1–12.

Jerolmack, D. J., and T. A. Brzinski (2010), Equivalence of abrupt grain-size transitions in alluvial rivers and eolian sand seas: A hypothesis, *Geology*, *38*(8), 719–722, doi:10.1130/G30922.1.

Jerolmack, D., D. Mohrig, J. Grotzinger, D. Fike, and W. Watters (2006), Spatial grain size sorting in eolian ripples and estimation of wind conditions on planetary surfaces: Application to Meridiani Planum, Mars, *J. Geophys. Res.*, *111*, E12S02, doi:10.1029/2005JE002544.

Kocurek, G., M. Carr, R. Ewing, K. Havholm, Y. Nagar, and A. Singhvi (2007), White Sands Dune Field, New Mexico: Age, dune dynamics and recent accumulations, *Sediment. Geol.*, *197*(3–4), 313–331, doi:10.1016/j.sedgeo.2006.10.006.

Krapivsky, P., and S. Redner (2007), Smoothing a rock by chipping, *Phys. Rev. E*, *75*(3), doi:10.1103/PhysRevE.75.031119.

Kuenen, P. H. (1960), Experimental Abrasion 4: Eolian Action, *J. Geol.*, *68*(4), 427–449, doi:10.1086/626675.

Lancaster, N. (1985), Winds and sand movements in the Namib sand sea, *Earth Surf. Processes Landforms*, *10*, 607–619, doi:10.1002/esp.3290100608.

Lancaster, N. (1995), *Geomorphology of Desert Dunes*, 290 pp., Routledge, London, doi:10.4324/9780203413128.

Langford, R. (2003), The Holocene history of the White Sands dune field and influences on eolian deflation and playa lakes, *Quaternary Int.*, *104*, 31–39, doi:10.1016/S1040-6182(02)00133-7.

Lewin, J., and P. Brewer (2002), Laboratory simulation of clast abrasion, *Earth Surf. Processes Landforms*, *27*, 145–164, doi:10.1002/esp.306.

Mazzullo, J., D. Eims, and D. Cunningham (1986), The effects of eolian sorting and abrasion upon the shapes of fine quartz sand grains, *J. Sediment. Petrol.*, *56*(1), 45–56.

McKee, E. D. (1966), Structures of dunes at White Sands National Monument, New Mexico (and a comparison with structures of dunes from other selected areas), *Sedimentology*, *7*(1), 3–69, doi:10.1111/j.1365-3091.1966.tb01579.x.

McKee, E. D., and J. R. Douglass (1971), Growth and movement of dunes at White Sands National Monument, New Mexico, *U.S. Geol. Surv. Prof. Pap.*, *750-D*, 108–114.

McLaren, P., and D. Bowles (1985), The effects of sediment transport on grain-size distributions, *J. Sediment. Petrol.*, *55*(4), 457–470.

Nalpanis, P., J. Hunt, and C. Barrett (1993), Saltating particles over flat beds, *J. Fluid Mech.*, *251*, 661–685, doi:10.1017/S0022112093003568.

Namikas, S., and D. Sherman (1997), Predicting aeolian sand transport: Revisiting the White model, *Earth Surf. Processes Landforms*, *22*(6), 601–604, doi:10.1002/(SICI)1096-9837(199706)22:6<601::AID-ESP783>3.0.CO;2-5.

Nickling, W. (1988), The initiation of particle movement by wind, *Sedimentology*, *35*(3), 499–511, doi:10.1111/j.1365-3091.1988.tb01000.x.

Nishimura, K., and J. C. R. Hunt (2000), Saltation and incipient suspension above a flat particle bed below a turbulent boundary layer, *J. Fluid Mech.*, *417*, 77–102, doi:10.1017/S0022112000001014.

Paola, C., P. Heller, and C. Angevine (1992), The large-scale dynamics of grain-size variation in alluvial basins. 1: Theory, *Basin Res. 4*, 73–90.

Pye, K., and H. Tsoar (2009), *Aeolian Sand and Sand Dunes*, Springer, Berlin.

Reitz, M. D., D. J. Jerolmack, R. C. Ewing, and R. L. Martin (2010), Barchan-parabolic dune pattern transition from vegetation stability threshold, *Geophys. Res. Lett.*, *37*, L19402, doi:10.1029/2010GL044957.

Rogers, J. J. W., and C. Schubert (1963), Size distributions of sedimentary populations, *Science*, *141*(3583), 801–802, doi:10.1126/science.141.3583.801.

Shao, Y., and H. Lu (2000), A simple expression for wind erosion threshold friction velocity, *J. Geophys. Res.*, *105*(D17), 22,437–22,443, doi:10.1029/2000JD900304.

Smalley, I., and C. Vita-Finzi (1968), The formation of fine particles in sandy deserts and nature of "desert" loess, *J. Sediment. Petrol.*, *38*(3), 766–774.

Spencer, D. W. (1963), The interpretation of grain size distribution curves of clastic sediments, *J. Sediment. Res.*, *33*(1), 180–190.

Warren, A. (1979), Aeolian processes, in *Processes in Geomorphology*, edited by C. Embleton and J. Thornes, pp. 325–351, Edward Arnold, London.

White, B. R. (1979), Soil transport by winds on Mars, *J. Geophys. Res.*, *84*(B9), 4643–4651, doi:10.1029/JB084iB09p04643.

Willetts, B., M. Rice, and S. Swaine (1982), Shape effects in aeolian grain transport, *Sedimentology*, *29*(3), 409–417, doi:10.1111/j.1365-3091.1982.tb01803.x.

Wolman, M., and J. Miller (1960), Magnitude and frequency of forces in geomorphic processes, *J. Geol.*, *68*(1), 54–74, doi:10.1086/626637.

Wright, J. (2001), Making loess-sized quartz silt: Data from laboratory simulations and implications for sediment transport pathways and the formation of 'desert' loess deposits associated with the Sahara, *Quaternary Int.*, *76–77*, 7–19, doi:10.1016/S1040-6182(00)00085-9.

Wright, J., and B. Smith (1993), Fluvial comminution and the production of loess-sized quartz silt: A simulation study, *Geogr. Ann., Ser. A*, *75*(1/2), 25–34, doi:10.2307/521050.

D. J. Jerolmack and R. L. Martin, Department of Earth and Environmental Science, University of Pennsylvania, Hadyen Hall, 240 S 33rd St., Philadelphia, PA 19104, USA. (sediment@sas.upenn.edu)

M. D. Reitz, Department of Physics and Astronomy, University of Pennsylvania, 209 S 33rd St., Philadelphia, PA 19104, USA.